

DISCLAIMER

This report was prepared as an account of work sponsored by an agency of the United States Government. Neither the United States Government nor any agency thereof, nor any of their employees, makes any warranty, express or implied, or assumes any legal liability or responsibility for the accuracy, completeness, or usefulness of any information, apparatus, product, or process disclosed, or represents that its use would not infringe privately owned rights. Reference herein to any specific commercial product, process, or service by trade name, trademark, manufacturer, or otherwise does not necessarily constitute or imply its endorsement, recommendation, or favoring by the United States Government or any agency thereof. The views and opinions of authors expressed herein do not necessarily state or reflect those of the United States Government or any agency thereof. Reference herein to any social initiative (including but not limited to Diversity, Equity, and Inclusion (DEI); Community Benefits Plans (CBP); Justice 40; etc.) is made by the Author independent of any current requirement by the United States Government and does not constitute or imply endorsement, recommendation, or support by the United States Government or any agency thereof.

Closing the Loop between In Situ Stress Complexity and EGS Fracture Complexity

A Bunger, Y Lu, F Fei, K Kroll Whiteside

October 2025



Disclaimer

This document was prepared as an account of work sponsored by an agency of the United States government. Neither the United States government nor Lawrence Livermore National Security, LLC, nor any of their employees makes any warranty, expressed or implied, or assumes any legal liability or responsibility for the accuracy, completeness, or usefulness of any information, apparatus, product, or process disclosed, or represents that its use would not infringe privately owned rights. Reference herein to any specific commercial product, process, or service by trade name, trademark, manufacturer, or otherwise does not necessarily constitute or imply its endorsement, recommendation, or favoring by the United States government or Lawrence Livermore National Security, LLC. The views and opinions of authors expressed herein do not necessarily state or reflect those of the United States government or Lawrence Livermore National Security, LLC, and shall not be used for advertising or product endorsement purposes.

This work performed under the auspices of the U.S. Department of Energy by Lawrence Livermore National Laboratory under Contract DE-AC52-07NA27344.

FORCE STRESS

1. Closing the loop between in situ stress complexity and EGS fracture complexity

- Organization or Affiliation: Lawrence Livermore National Laboratory
- Principal Investigator: Kayla A. Kroll
- Contact Information: krollwhitesi1@llnl.gov
- Subcontractors and/or Participating Organizations: Andrew P. Bunger, Associate Professor, University of Pittsburgh
- Project Start and End Dates: 03/2022 – 12/2025

2. Project Objectives and Purpose

The goal of the project is to integrate experimental true-triaxial block fracturing tests at high temperatures and high-fidelity numerical models to advance the understanding of the connection between in situ stress, wellbore orientation and hydraulic fracture patterns. Laboratory experiments aim to investigate the impact of various parameters including stress, temperature, and wellbore orientation on resulting fracture complexities near the wellbore. Rock properties to be used in numerical models are also measured in experiments. Numerical simulations focus on modeling various types of hydraulic fracturing across different scales and purposes, including minifrac tests or diagnostic fracture injection tests (DFITs), near-well hydraulic fractures, and far-field hydraulic stimulations. Simulation results are compared against experimental and/or field observations to validate the tools or infer the in situ stress condition in the Utah FORGE reservoir.

The project will have significant impacts on following aspects: (i) improving the in stress characterization at the Utah FORGE reservoir; (ii) offering a validated toolset in the open-source multi-physics simulation framework, GEOS, that will be available for future users; (iii) demonstrating the use of a suite of high-fidelity hydraulic fracturing simulation tools for EGS; (iv) providing a unique set of laboratory hydraulic fracturing experiments under both room temperature and high temperature to identify key components of in situ stress and to examine current technologies for stress estimation.

3. Technical Barriers and Targets

Technical barriers – the main technical barriers associated with the project goals include: (i) identifying the appropriate physics and numerical approaches to model hydraulic fracture nucleation and propagation at the relevant scale (from the near-well region to far field); (ii) characterizing the spatial profile of in situ stress and rock fabrics; (iii) performing hydraulic fracturing experiments using conditions that are relevant to Utah FORGE field applications; (iv) understanding how in situ stress, thermal effects, and wellbore orientations influence fracture patterns and how this information can be useful for stress estimation based on field data.

Technical targets – the main technical targets for Performance Period 3 include: (i) using the hydraulic fracturing model to simulate the minifrac test conducted at the production well, 16(B)78-32, during 2023; (ii) using the phase-field model to simulate the near-well hydraulic fracture pattern generated in both laboratory block fracturing experiments and field injection tests at Utah FORGE; (iii) using the hydraulic fracturing model to simulate far-field fracture propagation during Utah FORGE stimulations; (iv) perform laboratory block fracturing experiments under true triaxial compression for stress interpretation.

4. Technical Approach

The entire project is divided into four tasks, where Tasks 1-3 focus on modeling hydraulic fracture initiation and propagation across different scales and for various purposes, while Task 4 aims to perform block hydraulic fracturing experiments under true triaxial compression. We provide more detailed descriptions of the technical approach for each task below, primarily those methodologies adopted within Performance Period 3 (January – December, 2025).

Task 1 Numerical modeling of existing DFITs/minifrac tests

We employ a fully coupled finite-element/finite-volume hydraulic fracturing simulator in GEOS to model DFITs/minifrac tests. The entire simulation workflow consists of two stages: (1) simulation of fluid injection and hydraulic fracture propagation, and (2) simulation of the shut-in period and fracture closure based on the resulting fracture geometry and final injection pressure. Fracture propagation in the injection stage is modeled by an enhanced virtual crack closure technique (VCCT) based on linear elastic fracture mechanics (LEFM). Fracture closure in the shut-in stage is captured by incorporating a Barton-Bandis model in which a nonlinear relationship between the contact stress and hydraulic aperture is introduced. While we mostly considered a penny-shaped fracture in previous DFIT modeling, in this performance period, we switch to a PKN-like fracture with constrained height based on the image log observation and pressure records. To better match the post-closure pressure response in the field, a pressure-dependent matrix permeability model is also utilized to approximate potential effects of natural fractures during leak-off. Overall, this two-step workflow enables a more robust modeling of DFITs/minifrac tests and also facilitates understanding of pressure behavior in injection and shut-in stages individually. Mathematical formulations and solution procedures are detailed in [1].

Task 2 Phase-field modeling of near-well fracture complexity

This task uses an innovative phase-field model developed within this project to investigate the connection between in situ stress, wellbore orientation, and resulting near-well hydraulic fracture patterns. Fei et al. [2] provide the detailed formulation of the phase-field model and its key features, thus they are omitted here for brevity. In the past two years, the project focused on validating and calibrating the phase-field model based on Task 4 experiments and using the validated model to perform a comprehensive parameter study for the laboratory scale hydraulic fracturing test. In this performance period, we apply the model to simulate the near-well fracture nucleation and propagation in the minifrac test 2 (MF2) Cycle 1 on the production well, 16(B)78-32, and compare the simulation results with the post-test image log data. To study how near-well rock heterogeneity affects the fracture pattern, we generate a suite of heterogeneous rock property fields through a Gaussian-based geostatistical model based on the density log and sonic log data at the given depth. Different stress conditions and correlation lengths for the heterogeneous field are involved in the simulation to assess their effects on the resulting fracture pattern. Besides this field case study, we also continue the phase-field simulation for the laboratory scale hydraulic fracturing and investigate near-well hydraulic fracturing in a radially notched sample as prepared in Task 4. This simulation practice along with experimental tests aims to investigate the factors associated with the near-well fracture complexity in a well-controlled setup.

Task 3 Numerical modeling of far-field hydraulic fracturing

This task focuses on modeling far-field hydraulic fracturing at Utah FORGE, with the goal to infer far-field stress profile and relevant rock fabrics. We also employ the hydraulic fracturing module in GEOS for this task. Last year, we have performed simulations for the Stage 3 stimulation on the injection well, 16(A)78-32 and studied multiple model settings, including (i) uniform in situ stress gradient with isotropic rock toughness, (ii) uniform in situ stress gradient with anisotropic rock toughness to account for potential stress roughness, and (iii) non-uniform layered in situ stress profile with isotropic rock toughness. This year, we continue this Stage 3 modeling but consider a heterogeneous stress field to address a comment from one STAT reviewer in the Go/No-Go 2 meeting. The stress field is generated through a geostatistical model based on the input log data. Two main scenarios are studied: (i) an isotropic stress realization with identical correlation lengths in all x , y , and z directions; (ii) an anisotropic stress realizations with a larger correlation length in x and y directions than that in z . Figure 1 provides the slice view of corresponding heterogeneous stress profiles at a given x for both scenarios.

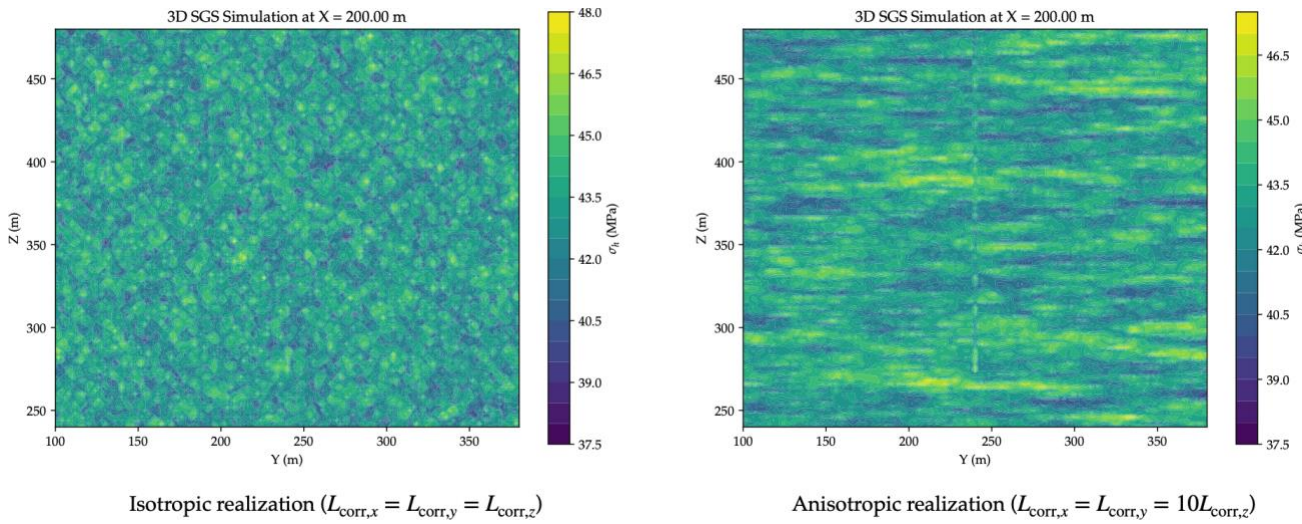


Figure 1 Comparison between the isotropic and anisotropic heterogeneous stress profiles for far-field hydraulic fracturing simulations at $x = 200$ m in the local coordinate.

Task 4 Laboratory hydraulic fracturing experiments

This task performs hydraulic fracturing experiments on 6-inch cubic granite samples under FORGE relevant conditions (temperature up to 200 °C), covering eight stress conditions, well directions, and well conditions (intact v.s. notched), different pressurized zones, and thermal stress situations. For each experiment, we obtain laboratory G -functions with both holistic and compliance methods, step-rate results, and fracture reopening measurements. These metrics are designed to improve the identification of key in situ stress components. After testing, each sample is first examined for the fracture pattern on the block surface and then over-cored to observe near-well fracture patterns. For some samples, we further process the over-cored section using SEM to observe the inner surface of the wellbore. Indirect tensile tests are also performed on Charcoal granite to study the tensile strength anisotropy in three principal directions.

5. Project Timeline (list milestones achieved and/or decision points)

Performance Period 1:

- Completed milestones: 1.1.1, 2.1.1, 3.1.1, 4.1.1, 4.2.1
- Go/No-Go decision achieved: G1, G2, G3 (passed in February, 2024)

Performance Period 2:

- Completed milestones: 2.2.1, 3.2.1, 4.4.1
- Go/No-Go decision achieved: G4, G5, G6 (passed in December, 2024)

Performance Period 3:

- Milestone 1.2.1: Completed results of THM modeling of Utah FORGE injection tests from 2021-2022 delivered and submitted (estimated completion: 12/2025).
- Milestone 2.3.1: Complete baseline phase-field model to predict near-well damaging and fracture nucleation patterns (completion date: 06/2025).
- Milestone 3.3.1: Complete baseline GEOS model to predict far-field fracture trajectories (estimated completion: 09/2025).
- Milestone 4.5: Laboratory block experiments with 4 different combinations of stresses/fabrics and 3 different wellbore geometries completed (completion date: 10/2024).

6. Technical Accomplishments

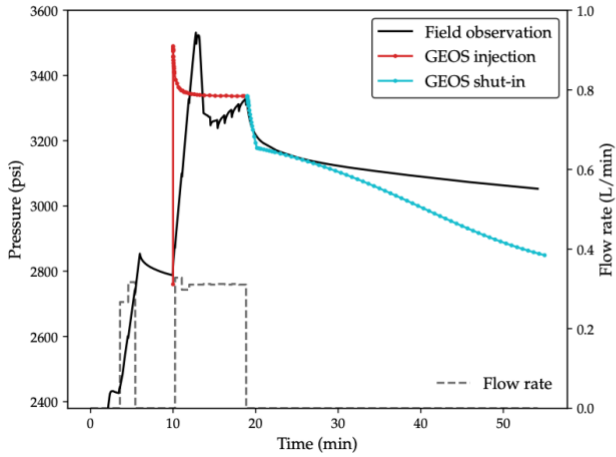
This work was performed under the auspices of the U.S. Department of Energy by Lawrence Livermore National Laboratory under Contract DE-AC52-07NA27344.

We summarize the main technical accomplishments achieved so far for each task in Performance Period 3 below.

Task 1 Numerical modeling of existing DFITs/minifrac tests

We have employed the modeling workflow to model MF2 Cycle 1 on the 16(B)78-32 well. To begin, we consider a baseline DFIT model with a PKN-like hydraulic fracture, constant matrix permeability, and the minimum horizontal stress $S_{hmin} \approx 21.91$ MPa or 3178 psi inferred from field data [3]. For the injection stage, we have studied the effects of maximum fracture height h_{max} , rock toughness K_{lc} , and S_{hmin} on the breakdown pressure and final injection pressure. We found that with $S_{hmin} = 21.91$ MPa, the calibrated $h_{max} = 2$ m and $K_{lc} = 1$ MPa·m^{1/2} lead to the injection pressure curve that reasonably matches field data, as can be seen in Figure 2(a), although the simulation shows a decreasing pressure after breakdown while the field data exhibits an increasing trend. The resulting fracture geometry and pressure are transferred to the shut-in stage for modeling fracture closure. Figure 2(a) presents the shut-in pressure curve with constant bulk permeability $k = 10^{-16}$ m², and reference aperture $w_0 = 1$ mm and reference normal stress $\sigma_{ref} = 10$ MPa for the Barton–Bandis model. It is noted that with calibrated parameters, the modeled fracture pressure agrees well with the field data in the first ten minutes after shut-in, but then it dissipates faster than the field measurement. One possibility is the induced hydraulic fracture intersects with natural fractures, thus the leakoff during shut-in may exhibit a pressure-dependent behavior. To explore this, we consider pressure-dependent matrix permeability following an exponential function [4]. As shown in Figure 2(b) **Error! Reference source not found.**, the modeled fracture pressure with this pressure-dependent permeability better matches the field observation, suggesting potential leakoff into natural fractures.

(a) Constant matrix permeability



(b) Pressure-dependent matrix permeability

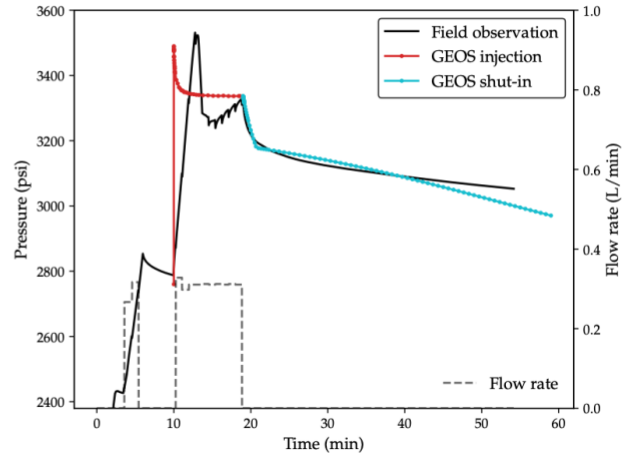
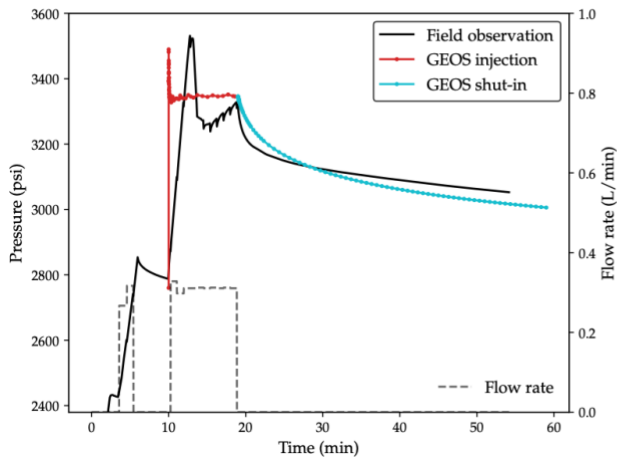


Figure 2 Comparison between the field data and GEOS modeling results for the case with (a) constant permeability, and (b) pressure-dependent permeability, when $S_{hmin} = 21.91$ MPa or 3178 psi, $K_{lc} = 1$ MPa·m^{1/2}, $h_{max} = 2$ m, $w_0 = 1$ mm, $\sigma_{ref} = 10$ MPa.

The above simulation assumes that S_{hmin} inferred from field observation is true. We also performed simulations with a different S_{hmin} to check if the inferred value from the field data is sufficiently accurate. To this end, we selected a smaller $h_{max} = 1$ m and calibrated $S_{hmin} = 20.61$ MPa and $K_{lc} = 2$ MPa·m^{1/2} to match the breakdown pressure and final pressure at the injection stage, as can be seen in Figure 3. This case presents a better result that it shows no pressure decay as observed in the first simulation with $S_{hmin} \approx 21.91$ MPa, which is opposite to the field observation. Subsequently, we import the results to the model for the shut-in stage with pressure-dependent permeability. With the calibrated permeability model, the modeled pressure well aligns with the field pressure. One key observation is the fracture still keeps open at the end of the simulation, while in the previous simulation, the fracture is closed when pressure drops to $S_{hmin} \approx 3178$ psi. Notably, we also don't see clear signal in the field pressure when the fracture is closed as the curve remains quite smooth throughout the shut-in period. Therefore, we hypothesize that the fracture is still open in the field test, and consequently, the inferred $S_{hmin} \approx 21.91$ MPa or 3178 psi from field data may overestimate the true value.

(a)



(b)

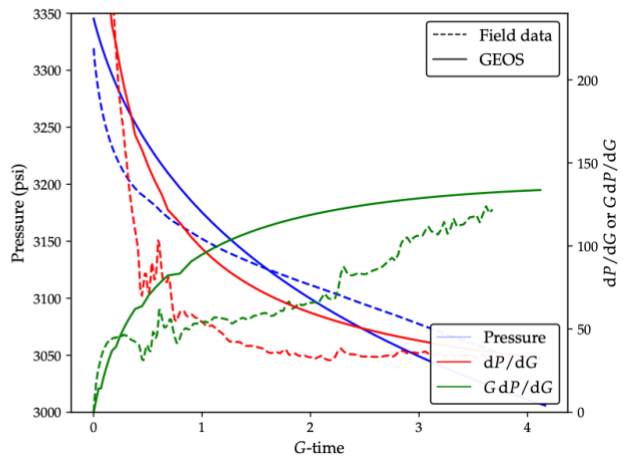


Figure 3 Comparison between the field data and GEOS modeling results in (a) evolution of pressure, and (b) G-function curves, for the case with $Sh_{min} = 20.61 \text{ MPa}$ or 2989 psi , $K_{lc} = 2 \text{ MPa} \cdot \text{m}^{1/2}$, $h_{max} = 1 \text{ m}$, $w_0 = 0.1 \text{ mm}$, $\sigma_{ref} = 10 \text{ MPa}$, and pressure-dependent permeability with $k_0 = 10^{-16} \text{ m}^2$.

Task 2 Phase-field modeling of near-well fracture complexity

We have conducted two phase-field modeling studies. The first work focuses on a baseline model for predicting near-well fracture nucleation and propagation. Specifically, we have applied our unique phase-field formulation with heterogeneous rock properties inferred from log data to model the near-well pattern of hydraulic fractures induced in MF2 Cycle 1 on the 16(B)78-32 well. Figure 4 presents the simulation results of near-well fracture patterns with following effective principal stress: $\sigma_{hmin} = 5 \text{ MPa}$, $\sigma_{hmax} = 15 \text{ MPa}$, $\sigma_v = 17.5 \text{ MPa}$. Three realizations of rock heterogeneities with different correlation lengths are considered. Compared to the case without heterogeneity, the simulation also produces bi-wing fractures in heterogeneous domains, and they are generally located at the azimuth that aligns with the σ_{hmax} direction and remain longitudinal to the wellbore. The difference is that the locations and heights of bi-wing fractures in the positive and negative σ_{hmax} directions become non-symmetric with heterogeneous fields. This non-symmetry is also observed in field image log, indicating the effects of rock heterogeneities on near-well fracture patterns. To study the influence of applied stress condition, we repeat the simulation with a lower $\sigma_{hmax} = 8 \text{ MPa}$, while other parameters are kept constant. Figure 5 shows the results with different correlation lengths. Clearly, the fracture pattern becomes more complex when the horizontal stress difference decreases, indicating that the near-well rock heterogeneity becomes more dominant. Also, the fracture pattern generally becomes more regular as the correlation length increases, or in other words, the rock becomes more uniform, which is expected.

Additionally, we employ the phase-field model to assist a recent experimental study on the notched sample in Task 4. Simulations with different notch depths, applied principal stresses, pressurized zone sizes have been conducted. Table 1 summarizes the geometry of induced hydraulic fractures for each condition.

Notch depth (mm)	Pressurized zone size = 50 mm		Pressurized zone size = 12.8 mm	
	$\sigma_{hmin} = 3 \text{ MPa}$	$\sigma_{hmin} = 7 \text{ MPa}$	$\sigma_{hmin} = 3 \text{ MPa}$	$\sigma_{hmin} = 7 \text{ MPa}$
1 mm	Radial circular	Radial + longitudinal	—	Longitudinal
2 mm	—	Radial circular	Radial non-circular	—
4 mm	—	Radial circular	—	—

Table 1 Summary of near-well fracture patterns obtained by the phase-field simulation of the notched sample.

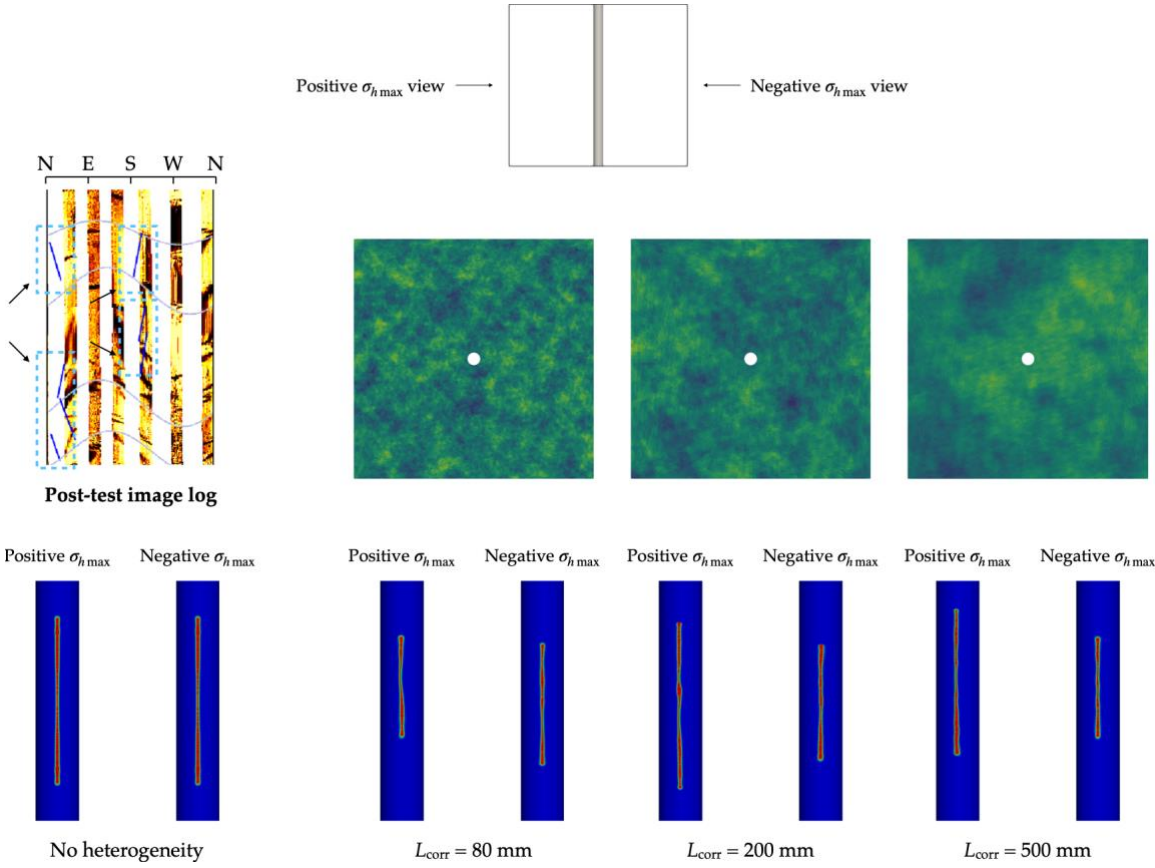


Figure 4 Phase-field simulations results of near-well fracture patterns for MF2 Cycle 1 on the 16(B)78-32 well with $\sigma_{h\min} = 5 \text{ MPa}$, $\sigma_{h\max} = 15 \text{ MPa}$, $\sigma_v = 17.5 \text{ MPa}$ and three different rock heterogeneity realizations.

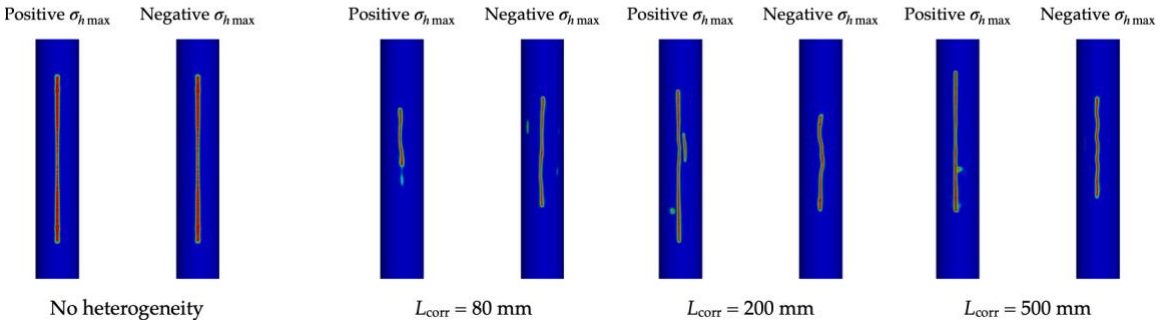


Figure 5 Phase-field simulations results of near-well fracture patterns for MF2 Cycle 1 on the 16(B)78-32 well with $\sigma_{h\min} = 5 \text{ MPa}$, $\sigma_{h\max} = 8 \text{ MPa}$, $\sigma_v = 17.5 \text{ MPa}$ and three different rock heterogeneity realizations.

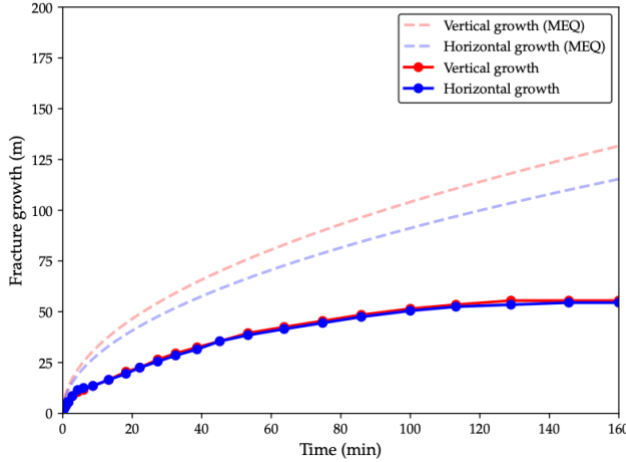
Task 3 Numerical modeling of far-field hydraulic fracturing

We have repeated the hydraulic fracturing simulation of Stage 3 with a heterogeneous stress field (Figure 1) inferred from the well log data. To begin, we consider a heterogeneous realization whose correlation lengths L_{corr} in all x , y , and z directions are identical. Figure 6(a) plots fracture propagation with time in both horizontal and vertical directions and their comparison with field observations inferred from microseismic data. As can be seen, with this heterogeneous stress profile, the simulation produces a much slower fracture propagation speed, while the previous simulation presented in the Go/No-Go 2 meeting with a “layered” stress profile can much better reproduce the fracture geometry inferred from the microseismic cloud. Therefore, we hypothesize that certain extent of anisotropy exists in the stress profile. Motivated by this, we create an anisotropic heterogeneous field with $L_{\text{corr},x} = L_{\text{corr},y} = 10L_{\text{corr},z}$, and

This work was performed under the auspices of the U.S. Department of Energy by Lawrence Livermore National Laboratory under Contract DE-AC52-07NA27344.

its simulation results are shown in Figure 6(b). Clearly, this case with an anisotropic stress profile performs much better in matching the field observation, indicating possible anisotropy in the in situ stress profile and corresponding rock fabrics.

(a) Isotropic realization ($L_{\text{corr},x} = L_{\text{corr},y} = L_{\text{corr},z}$)



(b) Anisotropic realization ($L_{\text{corr},x} = L_{\text{corr},y} = 10L_{\text{corr},z}$)

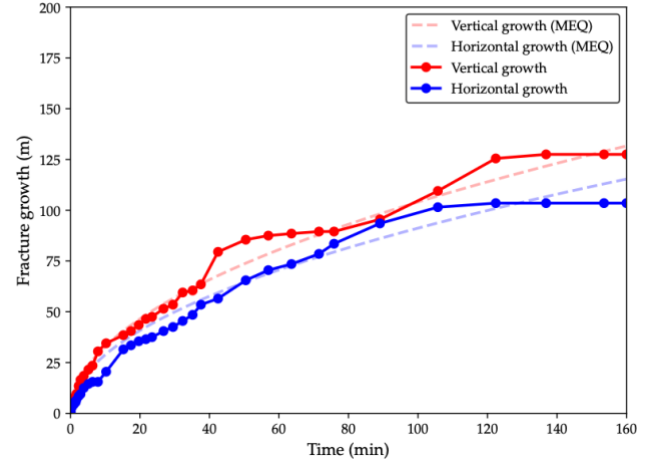


Figure 6 Comparison between the field data and simulation results for the hydraulic fracture growth in both horizontal and vertical directions with (a) isotropic stress heterogeneity, and (b) anisotropic stress heterogeneity.

Task 4 Laboratory hydraulic fracturing experiments

A total of 21 experiments have been conducted on 6-inch cubic granite samples. All completed tests can be categorized as follows based on well directions, presence of wellbore notch, and thermal stress conditions:

Category label	Full description
VR-NTS	Vertical well-Room temperature sample-Non-Thermal Stress
VH-NTS	Vertical well-High temperature sample-Non-Thermal Stress
VH-ITS	Vertical well-High temperature sample-Induced Thermal Stress
IH-ITS	Inclined well-High temperature sample-Induced Thermal Stress
HH-ITS	Horizontal well-High temperature sample-Induced Thermal Stress
HR-NTS	Horizontal well-Room temperature sample-Non-Thermal Stress
HR-NTS-N	Horizontal well-Room temperature sample-Non-Thermal Stress-Notched
HR-NTS-N-RPI	Horizontal well-Room temperature sample-Non-Thermal Stress-Notched-Reduced Pressurization

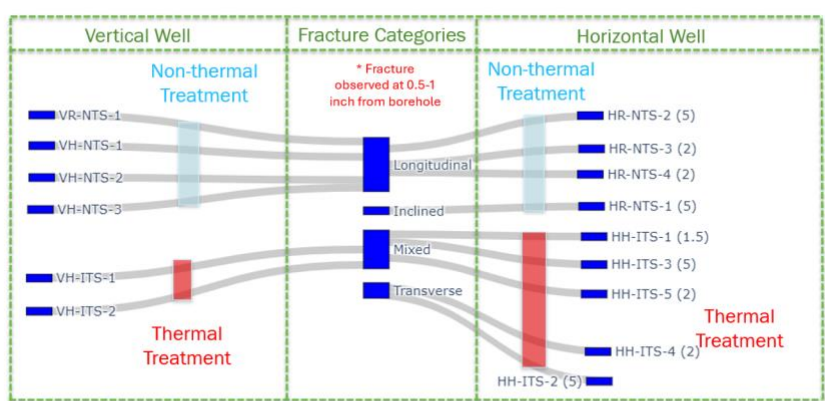
Results of each experiment category are summarized in Table 2 and Figure 7. These experimental datasets have provided evidence and insights for following questions during EGS development: (Q1) how circulation cooling affects the breakdown pressure; (Q2) how the thermal stress induced by cooling influences the fracture patterns; (Q3) what is the role of thermally induced micro-cracks in macro-fracture initiation and propagation; (Q4) How fracture segmentation and rock bridges influence fracture reopening and closure behavior, and the stress estimation.

Testing Case	Breakdown Pressure (Mpa)	Closure Pressure (MPa) -G function-Compliance Method	Closure Pressure (MPa) -G function-Holistic	Reopening Pressure (MPa)-Reopen	Reopening Pressure (MPa) - Step Rate	Applied Vertical Stress	Applied Horizontal Maximum Stress	Applied Horizontal Minimum Stress	Thermal Stress Effect	Notch
VR-NTS-1	18	--	--	--	17.5	15	10	N	N	
VH-NTS-1	23.2	14	7	14.2	7.8	17.5	15	10	N	N
VH-NTS-2	21.8	11	8	13.8	11.5	17.5	15	10	N	N
VH-NTS-3	22.4	13.5	11	22.5	15.8	17.5	15	10	N	N
VH-ITS-1	20.6	12	8	13.5	10	17.5	15	10	Y	N
VH-ITS-2	17.7	13	8	10	10.5	17.5	15	10	Y	N
HH-ITS-1	15.7	11.5	6.2	11	11	17.5	15	11.8	Y	N
HH-ITS-2	8.7	7	4	8.5	8.5	17.5	15	11.8	Y	N
HH-ITS-3	23.1	15	14	18	15.5	17.5	15	10	Y	N
HH-ITS-4	21.4	7.5	5.5	10	10	17.5	15	3	Y	N
HH-ITS-5	11	6	4	5	5	17.5	15	3	Y	N
HH-ITS-6	15	10	7	9	9	17.5	15	7	Y	N
HH-ITS-7	22.9	4	3	6	--	17.5	15	7	Y	N
HR-NTS-1	37.5	11	6.5	12	11	17.5	15	3	N	N
HR-NTS-2	42.5	11	7.8	14	13	17.5	15	3	N	N
HR-NTS-3	20.4	7.5	4.8	7	7	17.5	15	7	N	N
HR-NTS-4	23.2	12	9	12	11	17.5	15	7	N	N
HR-NTS-1-notch	37.8	13	9	20	13	17.5	15	7	N	2 mm
HR-NTS-2-notch	34.8	13	9	16	--	17.5	15	7	N	4 mm
HR-NTS-3-notch-shorten-injection	44.31	17.5	13.5	--	--	17.5	15	7	N	4 mm
HR-NTS-4-notch-shorten-injection	40.3	6	9	11	9	17.5	15	0.6	N	4 mm

Table 2 Summary of experiment results for eight combinations of testing conditions across 21 test.

1) Vertical well-Room temperature sample-Non-Thermal Stress (VR-NTS)
 2) Vertical well-High temperature sample-Non-Thermal Stress (VH-NTS)
 3) Vertical well-High temperature sample-Induced Thermal Stress (VH-ITS)

4) Horizontal well-High temperature sample-Induced Thermal Stress (HH-ITS)
 5) Horizontal well-Room temperature sample-Non-Thermal Stress (HR-NTS)



Transverse: fracture perpendicular to wellbore drilling direction

Longitudinal: fracture parallel to wellbore drilling direction

Mixed: Transverse and Longitudinal exist at the same time

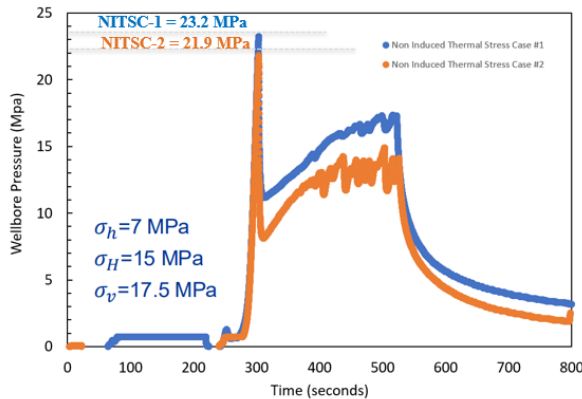
Inclined: Fracture angles with wellbore drilling direction range from 10 to 45 degrees.

Figure 7 Effects of wellbore orientation and thermal treatment on near-well fracture patterns for the un-notched case

For Q1, we have observed in most experiments and confirmed that thermal stress can lower the breakdown pressure as shown in Figure 8. For Q2, both vertical and horizontal wellbores have presented the influence of the thermal stress on the fracture patterns. For example, longitudinal fractures are observed for the horizontal well without cooling, which it transforms into a combination of transverse and longitudinal fractures due to the effects of thermal stress from cooling. For Q3, we plan to leverage the numerical simulation to study this by accounting for the thermally-induced micro-crack. Meanwhile, the post-test fractured sample remained intact for almost all experiments, even after over-core drilling. The SEM result shows that the fracture is not continues but contains multiple segmentations where the rock still remain intact, forming rock bridges. This observation is different from that in shale or sandstone and further stresses the importance of Q4. These rock bridges influence fracture reopening and closure response and consequently affect stress estimation from the DFIT analysis. Our current results indicate that even for

a simple planar radial fracture under controlled laboratory conditions, neither the holistic nor the compliance method can provide an accurate estimate of horizontal stress.

Non Induced Thermal Stress Group



Induced Thermal Stress Group

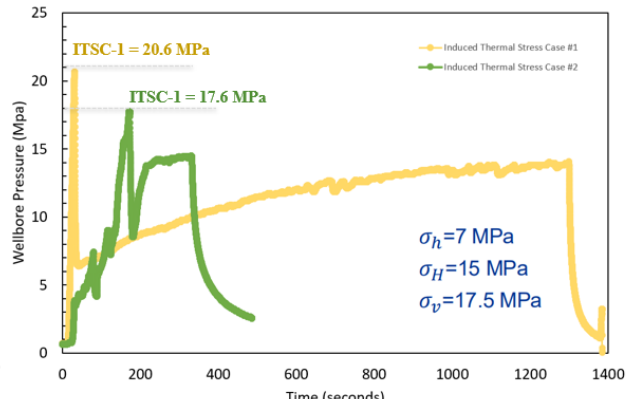


Figure 8 Breakdown pressure comparison between the non-thermal (left) and the thermal treatment (right) with the same wellbore and stress conditions.

7. Challenges to Date

Major challenges or variances are summarized below for Performance Period 3.

- DFIT/minifrac test modeling: The original plan is to model injection tests during 2021-2022. However, no documented injection test or comprehensive dataset were found for this period. Therefore, we decided to study the minifrac tests on the 16(B)78-32 well conducted in 2023. Most importantly, these minifrac tests have offered sufficient data and reports to define modeling setup.
- Experiment: The difficulties of granite preparation and post-processing due to its unique mechanical properties introduced additional cost and increased labor and time, resulting the challenge for repeatability. To address this, we have improved experimental design and calculations to determine the optimal test conditions. Consequently, we are able to perform more repeated experiments and generate a solid database that allows for systematic investigation.

8. Conclusion and Plans for the Future

Conclusions for each task are summarized below:

- *Task 1:* We have conducted numerical DFIT modeling for the minifrac test conducted on the 16(B)78-32 well. Two key observations were obtained from the numerical study. First, the simulation result implies a pressure-dependent fluid leakoff behavior, suggesting potential influence from natural fractures. Also, the simulation also indicates certain f still remains open at the end of the test, indicating that the minimum horizontal stress inferred from the field data may be overestimated.
- *Task 2:* We have demonstrated the capability of the phase-field formulation developed within this project to predict near-well fracture/damage patterns for field injection tests in the presence of rock heterogeneity. Simulations of both field tests and laboratory tests highlight the standout feature of the phase-field model in handling complex fracture geometries in this near-well region.
- *Task 3:* We have extended the previous numerical study on Stage 3 by incorporating a heterogeneous stress field. Simulation results with different heterogeneity realizations indicate certain degree of anisotropy in the field stress profile based on the comparison between modeled hydraulic fractures and microseismic data. Through this simulation study, we also demonstrate the capability of the hydraulic fracturing simulator in GEOS to model far-

field fracture growth that involved stress gradient, stress heterogeneity, apparent toughness anisotropy, and size-dependence of toughness.

- *Task 4:* We have provided a large number of comprehensive experimental data to support simulations, field design and data interpretation. More importantly, this work has offered ample experience and guidance for future EGS experiment design, especially on the granite hydraulic fracturing test at high temperature. Also, the

Before the end of the project, we will have following plans

- Continue the DFIT simulation for MF2 Cycle 1 on the 16(B)78-32 well by involving thermal effects, i.e., thermal stress on the fracture due to cooling.
- Prepare the publication(s) for combined experimental and numerical study on Tasks 2 & 4.
- If time allows, we will apply the far-field hydraulic fracture simulation to more recent stimulations on 16(A)78-32 and 16(B)78-32 wells. The potential difficulty is the microseismic data for these stages seem to suggest significant impacts of natural fractures and also interactions between stimulated fractures at different stages. Therefore, it will introduce great complexity to characterize the in situ stress profile alone.
- Perform additional tests with two wellbore inclinations by the end of project. If time and budget allow, we will focus on (i) studying how thermal stresses and thermally induced fractures during pre-circulation affect resulting fracture patterns, and (ii) revisiting the G -function theory and incorporating fracture segmentation effects to make the theory more suitable for granite in EGS applications.

9. Geothermal Data Repository

[TODO]

10. Publications and Presentations, Intellectual Property (IP), Licenses, etc.

- [1] F. Fei, Y. Lu, A. Bunger, M. Cusini, Connecting In Situ Stress to Near-well Hydraulic Fracture Complexity with Phase-field Simulations. 2025 Biot Conference.
- [2] F. Fei, Y. Lu, A. Bunger, M. Cusini, A Numerical Study of Hydraulic Fracturing Experiments for In Situ Stress Characterization in Enhanced Geothermal Systems (EGS). 2024 Geothermal Rising Conference.
- [3] Y. Lu, F. Fei, M. Cusini, A. Bunger, Understanding Impact of Complex Fracture Patterns in EGS In situ Stress Estimations Through Post-Peak Pressure Analysis from High-Temperature True-Triaxial Block Fracturing Experiments. 2024 Geothermal Rising Conference.
- [4] Modeling of Diagnostic Fracture Injection Tests (DFITs) for In situ Stress Characterization in the Utah FORGE Reservoir, 49th Workshop on Geothermal Reservoir Engineering Stanford University, Stanford, California, February 12-14, 2024.
- [5] Y. Lu, G. Lu, F. Fei, M. Cusini, A. Bunger, Understanding In situ Stress Complexities in EGS Reservoirs through True-Triaxial Block Fracturing Experiments on High Temperature Analogue Utah FORGE Granites, 2023 GRC.
- [6] F. Fei, A. Costa, J.E. Dolbow, R.R. Settgast, M. Cusini, A phase-field model for hydraulic fracture nucleation and propagation in porous media, *Int J Numer Anal Methods*. 2023; 47: 3065–3089.
- [7] F. Fei, A. Costa, J.E. Dolbow, R.R. Settgast, M. Cusini, Phase-field modeling of hydraulic fracture nucleation and propagation in rocks, oral presentation at *USNCCM 2023*.
- [8], F. Fei, A. Costa, J.E. Dolbow, R.R. Settgast, M. Cusini, Phase-field modeling of hydraulic fracturing under heterogeneities and/or anisotropies of rock properties and in situ stress, *ARMA US Rock Mechanics/Geomechanics Symposium*, 2023.
- [9] F. Fei, A. Costa, J.E. Dolbow, R.R. Settgast, M. Cusini, Phase-field simulation of near-wellbore nucleation and propagation of hydraulic fractures in enhanced geothermal systems (EGS), *Proceedings of the SPE Res. Sim. Conf.*, Galveston, Texas, USA, March 2023.
- [10] F. Fei, Y. Lu, A. P. Bunger, M. Cusini, Experimental and Numerical Study of Hydraulic Fracturing in Enhanced Geothermal Systems, 48th Workshop on Geothermal Reservoir Engineering, Stanford University, Stanford, California, February 6-8, 2023.

References

1. Fei, F., et al. *Modeling of Diagnostic Fracture Injection Tests (DFITs) for In-situ Stress Characterization in the Utah FORGE Reservoir*. in *49th Workshop on Geothermal Reservoir Engineering*. 2024. Stanford University, Stanford, California, USA.
2. Fei, F., et al., *A phase-field model for hydraulic fracture nucleation and propagation in porous media*. *International Journal for Numerical and Analytical Methods in Geomechanics*, 2023. **47**(16): p. 3065-3089.
3. Kelley, M., et al., *Utah FORGE 2439: Report on Minifrac Tests for Stress Characterization*. 2024: Geothermal Data Repository, Battelle Memorial Institute, <https://gdr.openei.org/submissions/1596>.
4. Lee, S.H. and A. Ghassemi. *Modeling and Analysis of Stimulation and Fluid Flow in the Utah FORGE Reservoir*. in *48th Workshop on Geothermal Reservoir Engineering*. Stanford University, Stanford, California, USA.